http://dx.doi.org/10.5935/0103-5053.20140136

J. Braz. Chem. Soc., Vol. 25, No. 8, 1528-1535, 2014.
Printed in Brazil - ©2014 Sociedade Brasileira de Química
0103 - 5053 $6.00+0.00

Article

Spectroscopic, Electrochemical, Magnetic and Structural Investigations of Dimanganese-(II/II) and Mixed-Valence-(II/III)-Tetraiminodiphenolate Complexes

Julio C. da Rocha,[a] Giordano Poneti,[b,c] Janaina G. Ferreira,[a] Ronny R. Ribeiro[a] and Fábio S. Nunes*[*,a]

[a]*Departamento de Química, Universidade Federal do Paraná, CP 19081, 81531-990 Curitiba-PR, Brazil*

[b]*Laboratory of Molecular Magnetism (LAMM), Department of Chemistry, Ugo Schiff and INSTM Research Unit, University of Florence, Via della Lastruccia, 3-13, 50019 Sesto Fiorentino, Florence, Italy*

[c]*Department of Applied Science and Technology, "Guglielmo Marconi" University, Via Plinio 44, 00193 Rome, Italy*

Neste trabalho descrevemos a preparação e a caracterização espectroscópica [ressonância paramagnética eletrônica (EPR), espectroscopia UV-Vis e espectroscopia de infravermelho com transformada de Fourier (FTIR)], magnética e espectroeletroquímica do complexo $[Mn^{II}_2(tidf)(OAc)(ClO_4)(MeOH)]$ (tidf = ligante macrocíclico do tipo Robson, obtido pela condensação entre 2,6-diformil-4-metilfenol e 1,3-diaminopropano). O composto $[Mn^{II}_2(tidf)(OAc)(ClO_4)(MeOH)]$ exibe antiferromagnetismo fraco e constante de acoplamento magnético $J = -1.59(1)$ cm^{-1}. A oxidação de $[Mn^{II}_2(tidf)(OAc)(ClO_4)(MeOH)]$ monitorada por experimentos de espectroeletroquímica de UV-Vis e de EPR produziu espécies de valência mista Mn_2(II/III) com perfil espectral semelhante ao do complexo $[Mn^{II}Mn^{III}(tidf)Br_3(H_2O)_2]$. Tentativas de cristalização de $[Mn^{II}_2(tidf)(OAc)(ClO_4)(MeOH)]$ produziram o complexo trinuclear de manganês $[Mn_3{}^{III/II/III}(tidf)_2(\mu\text{-}OAc)_2](ClO_4)_2$. O composto possui duas unidades $[Mn^{III}(tidf)]^+$ onde o íon metálico é pentacoordenado e conectadas a um íon central de Mn^{II} hexacoordenado através de pontes μ-fenolato e μ-acetato.

Synthesis, spectroscopic [electron paramagnetic resonance (EPR), UV-Vis and Fourier transform infrared spectroscopy (FTIR)], magnetic and spectroeletrochemical properties of $[Mn^{II}_2(tidf)(OAc)(ClO_4)(MeOH)]$ (tidf = a Robson type macrocyclic ligand obtained through condensation of 2,6-diformyl-4-methylphenol and 1,3-diaminopropane) are reported. Compound $[Mn^{II}_2(tidf)(OAc)(ClO_4)(MeOH)]$ shows a weak antiferromagnetic behavior with exchange coupling constant $J = -1.59(1)$ cm^{-1}. UV-Vis and EPR spectroelectrochemical response after oxidation of complex $[Mn^{II}_2(tidf)(OAc)(ClO_4)(MeOH)]$ detected the stabilization of mixed-valence Mn_2(II/III) species in solution showing spectral features similar to the ones of the isolated mixedvalence $[Mn^{II}Mn^{III}(tidf)Br_3(H_2O)_2]$ compound. Crystallization of $[Mn^{II}_2(tidf)(OAc)(ClO_4)(MeOH)]$ surprisingly produced the trimanganese complex $[Mn_3{}^{III/II/III}(tidf)_2(\mu\text{-}OAc)_2](ClO_4)_2$, not observed in solution. It contains two pentacoordinated $[Mn^{III}(tidf)]^+$ units, each one connected to a central hexacoordinated Mn^{II} ion through one μ-phenolate and one μ-acetate bridge.

Keywords: dimanganese macrocyclic complexes, tetraiminodiphenolate, magnetic properties, spectroeletrochemistry, crystal structure

Introduction

Dicompartment macrocycles, like the tetraiminodiphenolate (tidf) seen in Scheme 1, are very attractive molecules for their ability to bind two metal ions such as vanadium, manganese, iron, cobalt, nickel, copper, zinc and ruthenium.[1-16] Those compounds have been widely used as building blocks to the rational design and preparation of polynuclear complexes with specific supramolecular architectures and magnetic properties.[17-23] Using tidf

*e-mail: fsnunes@ufpr.br

ligand, we have recently reported on the synthesis, crystal structure, spectral, magnetic and electrochemical properties of some homometallic and heterometallic complexes, such as $[\{Cu_2(tidf)(H_2O)\}_2(\mu\text{-}CN)_2Fe(CN)_4]\cdot 6H_2O$, $[Cu_2(tidf)(H_2O)_2][Ni(CN)_4]$, $[Cu_2(tidf)(H_2O)_2][Fe(CN)_5NO]\cdot H_2O$,[3] $[Co_2(tidf)(ClO_4)_2(H_2O)_2]$,[4] $[Fe_2(tidf)(MeOH)_4](ClO_4)_2$,[9] $[Ru_2(tidf)Cl_2(H_2O)_2]\cdot H_2O$ and $[Ru(MeOH)_2FeCl(H_2O)(tidf)](ClO_4)$.[6] Manganese compounds, in addition, have been intensively studied by chemists due to their rich redox chemistry. Dimanganese complexes continue to be intensively studied as bioinorganic models for important enzymes such as catatales, for instance.[24]

Herein we report on the spectral, magnetic and electrochemical properties of the binuclear $[Mn^{II}_2(tidf)(OAc)(ClO_4)(MeOH)]$ (**1**) complex and on the single-crystal structure of a new and unusual trinuclear manganese(III/II/III) compound, $[Mn_3(tidf)_2(\mu\text{-}OAc)_2](ClO_4)_2$.

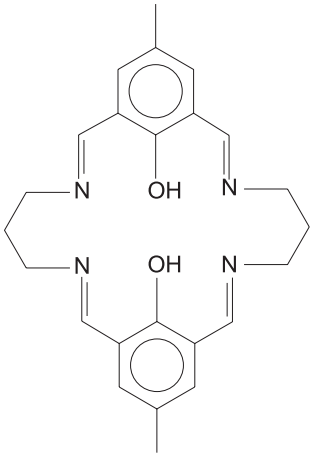

Scheme 1. Ligand tidf.

Experimental

Synthesis

The following preparations were carried out under inert atmosphere using Schlenk techniques.

$[Mn^{II}_2(tidf)(OAc)(ClO_4)(MeOH)]$ (**1**)

2.5 mL (30.5 mmol) of 1,3-diaminopropane were mixed with 11 g (30.5 mmol) of $Mn(ClO_4)_2\cdot 6H_2O$ and 7.5 g (30.5 mmol) of $Mn(OAc)_2\cdot 4H_2O$ in 50 mL of methanol. To this solution was added 5 g (30.5 mmol) of 2,6-diformyl 4-methyl formol dissolved in 150 mL of hot methanol. The resulting dark-brown solution was refluxed for 2 h. A microcrystalline yellow solid was recovered by filtration, washed with methanol and dried under vacuum. Yield was 4.5 g (44%). Elemental analysis for $C_{27}H_{33}ClMn_2N_4O_9$ (702.90): C, 46.14; H, 4.73; N, 7.97%. Found: C, 45.86; H, 4.20; N, 8.08%. IR (KBr pellet) cm^{-1}: 1627 *vs*. (ν C=N), 1582 s $n_{as}(CO_2^-)_{acetate}$, $n_s(CO_2^-)_{acetate}$ is masked, 1558 s (ν C=C), 1323 m (ν C–O)$_{phenolate}$, 1109 s and 623 m (ν Cl–O), 580 vw (ν Mn–N), 507 w (ν Mn–O).

$[Mn^{II}Mn^{III}(tidf)Br_3(H_2O)_2]$ (**2**)

A solution was prepared dissolving 3 g (18 mmol) of 2,6-diformyl 4-methyl formol and 6.5 g (18 mmol) of $Mn(ClO_4)_2\cdot 6H_2O$ in 90 mL of methanol. To this, was added 1,3-diaminopropane (1.5 mL, 18 mmol) and 2.5 mL (18 mmol) of triethylamine dissolved in 10 mL of methanol. After 2 h of reflux, 2.1 g (2.8 mmol) of a yellow solid, $[Mn_2(tidf)(ClO_4)_2(H_2O)_2]$, was recovered by filtration. This compound is very sensitive to oxidation and was immediately used to prepare the mixed-valence complex. $[Mn_2(tidf)(ClO_4)_2(H_2O)_2]$ was added to a bromine solution prepared from 0.15 mL (2.8 mmol) of 99.5% Br_2 in 250 mL of MeCN and kept under stirring for 2 h at room temperature. After workup, a brown-greenish solid was isolated, and dried under vacuum. Yield 1.0 g (47%). Elemental analysis for $C_{24}H_{30}Br_3Mn_2N_4O_4$ (788.11): C, 36.58; H, 3.84; N, 7.11%. Found: C, 36.95; H, 3.95; N, 6.67%. IR (KBr pellet) cm^{-1}: 1631 *vs.* (ν C=N), 1555 s (ν C=C), 1325 m (ν C–O), a set of small bands overlaid below 800 cm^{-1} precluded any unambiguous assignment of the metal-ligand vibrational modes.

$[Mn_3^{III/II/III}(tidf)_2(\mu\text{-}OAc)_2](ClO_4)_2$ (**3**)

Complex $[Mn^{II}_2(tidf)(OAc)(ClO_4)(MeOH)]$ (**1**) was dissolved in dichloromethane. Slow diffusion of toluene over the solution produced yellow needles suited for X-ray crystallography. The crystals were isolated and washed with diethyl ether.

Physical measurements

UV-Vis spectra in the range 190-900 nm were obtained on a VARIAN Cary 100 spectrophotometer in acetonitrile. Infrared spectra were obtained with a FTS3500GX Bio-Rad Excalibur series spectrophotometer in the region 4000-400 cm^{-1} in KBr pellets. The electron paramagnetic resonance (EPR) spectra from powdered solid samples were recorded on a Bruker Elexsys E500 X-band spectrometer. The 77 K spectra were obtained employing a quartz finger Dewar.

Magnetic investigations were performed on powdered samples using a Quantum Design MPMS instrument equipped with a 5 T magnet. The temperature dependence of the magnetization (M) was followed from 1.8 to 300 K by applying a 10 kOe field (H) from 300 to 45 K and a 1 kOe field below 45 K to reduce magnetic saturation effects.

Magnetic susceptibility per mole (χ_M) was then evaluated as $\chi_M = M_M/H$. Magnetic data were corrected for the sample holder contribution and for the sample diamagnetism using Pascal's constants ($c_{dia} = 3.21 \times 10^{-4}$ emu mol^{-1}).[25]

Cyclic voltammetry was carried out with an IVIUM CompactStat potentiostat/galvanostat. A platinum disc electrode was employed for the measurements at I = 0.1 mol L^{-1} kept constant with tetrabutylammonium hexafluorophosphate ($TBAPF_6$). A $Ag/AgNO_3$ ([Ag^+] = 0.01 mol L^{-1} in a MeCN solution of $TBAPF_6$ 0.1 mol L^{-1}) along with a platinum wire were used as reference (0.503 V *vs.* SHE) and auxiliary electrodes, respectively. Typical experiments were conducted with a 3.0×10^{-3} mol L^{-1} complex concentration in acetonitrile, DMF and methanolic solutions at ambient temperature.

UV-Vis spectroelectrochemistry measurements were performed with the IVIUM CompactStat potentiostat/galvanostat attached to a Agilent 8453 diode-array spectrophotometer from ca. 1 mmol L^{-1} complex and 0.1 mol L^{-1} $TBAPF_6$ acetonitrile solutions. A three electrode system was used with a thin layer cell of 0.1 cm internal optical path length. A platinum minigrid was used as transparent working electrode, in the presence of a small $Ag/AgNO_3$ reference electrode and a platinum auxiliary electrode.

EPR spectroelectrochemistry was accomplished using the chronoamperometric mode in a two-electrode configuration glass cell containing platinum working and $Ag/AgNO_3$ reference electrodes. Approximately 1 mL of the complex solution was electrolyzed under stirring at 1.0 V for 30 min, after which no current was developed. After, 200 μL of the sample was transferred to a quartz tube and the EPR spectrum taken at 77 K.

The X-ray data were collected using a Bruker diffractometer, equipped with Cu Kα radiation (ImuS source). Cell refinement and data reduction were done using APEX2.[26] Absorption corrections were applied using SADABS.[26] Structure was solved by direct methods using SIR2004[27] and refined on F^2 by full-matrix least squares using SHELXL97.[28] All non hydrogen atoms were refined anisotropically. The complex shows a disorder effect at the perchlorate anion and co-crystallizes with solvent molecules in the unit cell. The disordered anion molecule was refined using appropriate restraints. The structure refinement with the solvent molecules in the cell is not satisfactory. In consequence, the squeeze procedure was adopted.[29] Drawings were made with the ORTEP-3 for Windows.[30] More detailed information about the structure determinations is given in Table 1. Microanalyses were done in a CHN-2400 Perkin-Elmer analyzer.

Table 1. Crystal data and structure refinement for the $[Mn_3(tidf)_2(\mu\text{-}OAc)_2](ClO_4)_2$

Empirical formula	$C_{52}H_{58}Cl_2Mn_3N_8O_{16}$
Formula weight	1286.78
T / K	150
Wavelength / Å	1.54184
Crystal system, space group	Triclinic
Unit cell dimensions	a = 12.7279(8) Å α = 70.836(4)°
	b = 16.473(1) Å β = 83.134(4)°
	c = 17.798(1) Å γ = 89.852(4)°
Volume / Å^3	3497.0(4)
Z, calculated density / (g cm^3)	2, 1.222
Absorption coefficient / mm^{-1}	5.561
F(000)	1326
Crystal size / mm	0.02 × 0.03 × 0.16
Theta range / degree	2.65-71.22
Index ranges	$-14 \le h \le 15$
	$-18 \le k \le 20$
	$0 \le l \le 21$
Reflections collected, Indep.	35994, 12648 (Rint 0.065)
Observed data [$I > 2\sigma(I)$]	8262
Completeness to theta max	0.928
Max. and min. transmission	0.753 and 0.432
Refinement method	Full-matrix least-squares on F^2
Data, restraints, parameters	12648, 30, 743
Goodness-of-fit on F^2	1.024
Final R indices [$I > 2\sigma(I)$]	R_1 0.0977
	wR_1 0.273
R indices (all data)	R_1 0.121
	wR_2 0.289
Largest diff. peak and hole (e.Å^3)	1.4 and −0.8

Results and Discussion

Spectroeletrochemistry

Figure 1a shows the UV-visible spectrum of complex **1** in acetonitrile. The intense bands at 217 and 254 nm are typical of intra-ligand π(tidf) → π*(tidf) with a higher contribution from the diphenolate groups while the transition at 370 has a similar assignment, but involving diimines functions.[31-33] The small shoulder at 386 nm is due to either MLCT or a LMCT transition. The low intensity shoulder observed at 465 nm can be tentatively assigned to a spin-forbidden d-d band.

Cyclic voltammograms of **1** in acetonitrile exhibited a single pair of waves in the −2.0 to 2.0 V window with E_{pa} = 0.14 V *vs.* Ag/Ag^+ and peak separation (ΔE_p) of 112 mV at 100 mV s^{-1} (Figure 1b), assigned to the

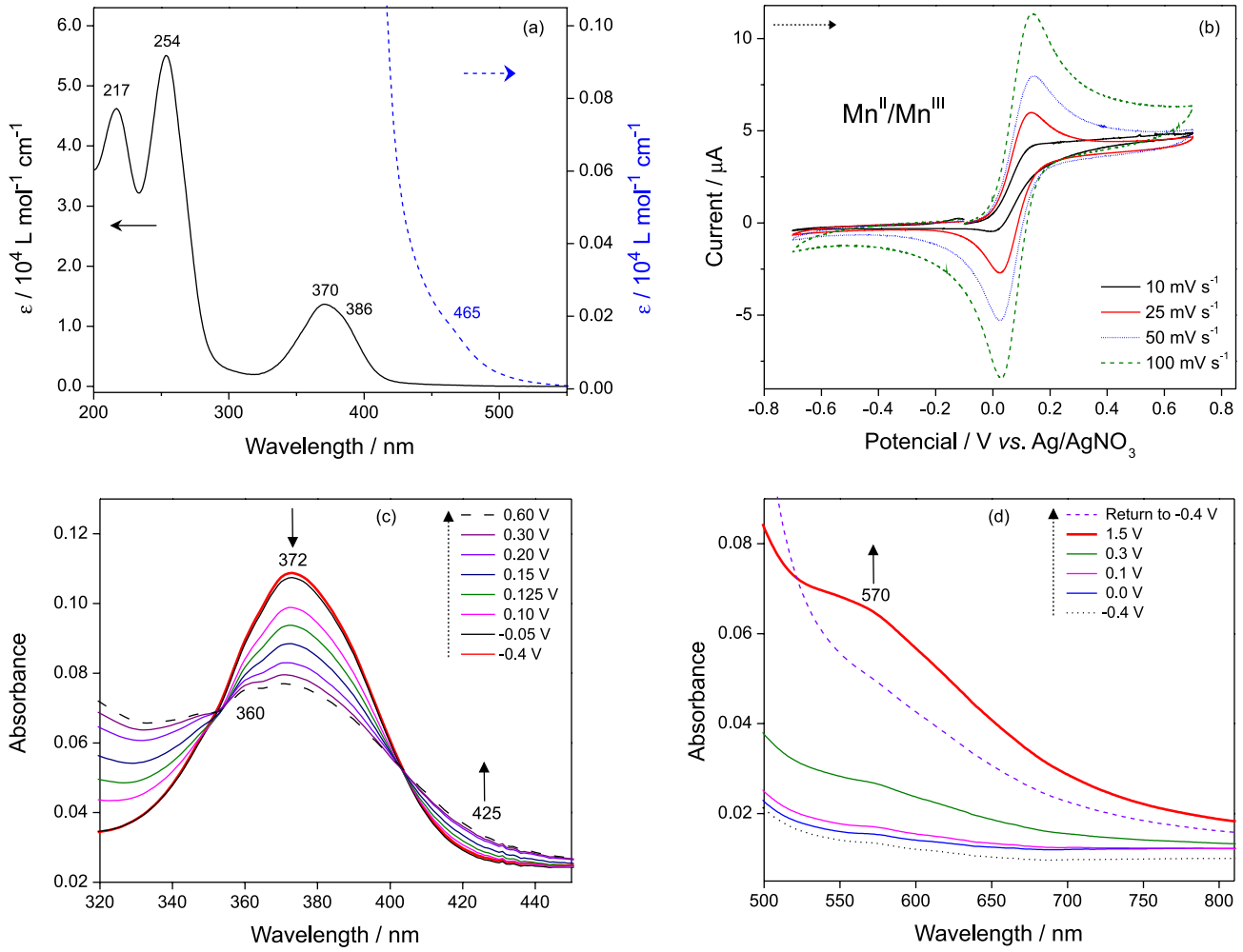

Figure 1. (a) UV-Vis spectrum of complex **1** in acetonitrile; (b) cyclic voltammogram of **1** in acetonitrile; (c) and (d) spectroelectrochemistry upon oxidation of **1** in acetonitrile. I = 0.10 mol L^{-1} $TBAPF_6$ in CH_3CN. Potentials *vs.* Ag/Ag^+ (0.503 V *vs.* SHE). The spectra were recorded after applying each potential for 30 s.

quasi-reversible electron transfer process $Mn_2^{II} \rightarrow Mn^{II}Mn^{III}$. Chang *et al*. also reported the monoelectronic oxidation of $[LMn_2^{II/II}Cl_2].1/2MeOH$ with $E_{1/2}$ = 0.093 V *vs*. Ag/Ag^+ (L = is the dianion of the Schiff base condensation of 2 mol of 1,3-diaminopropane and 2 mol of 2,6-diformyl-4-tert-butylphenol).[34] The magnesium complex $[Mg_2(tidf)_2(CH_3CN)_2]^{2+}$ undergoes an irreversible reduction between −1.10 and −1.50 V *vs.* Ag/Ag^+, which is related to the macrocyclic ligand tidf since the magnesium in not electroactive in that range of potential. Contrary to $[Mg_2(tidf)_2(CH_3CN)_2]^{2+}$, no intraligand redox processes were observed for $[Mn_2(tidf)(OAc)(H_2O)_2]^+$ in the same potential window, indicating a substantial electronic communication between the molecular orbitals of the manganese and the macrocycle ligand. This interaction is naturally reflected in the electronic spectra of the complex as we discuss below.

Spectroelectrochemical response of complex **1** between −0.40 and +1.50 V *vs.* Ag/Ag^+, seen in Figures 1c and 1d, shows the decrease in the intensity of the band at 372 nm, which is an intraligand $\pi \rightarrow \pi^*_{(diimine)}$ transition. Since the ligand does not show any electrochemical activity in this range, we can conclude that the band at 372 also contains some contribution from MLCT transitions. The bands below 300 nm exhibited a slight decrease in intensity, also in accordance with an electronic metal-ligand delocalization. Hence, a change in the electron density on the manganese ion upon oxidation influences the UV-Vis spectrum. The oxidation $Mn^{II} \rightarrow Mn^{III} + e^-$ was also followed by an increase of the absorbance at 425 nm (Figure 1c), most likely caused by a LMCT transition, $p\pi(tidf) \rightarrow d\pi Mn^{III}$, and at 570 nm (Figure 1d) assigned to a d-d transition. These features agree with the spectrum of the isolated mixedvalence complex $[Mn^{II}Mn^{III}(tidf)Br_3(H_2O)_2]$ (**2**) as shown in Figure 2.

In order to validate the oxidation numbers of the manganese ions after oxidation of complex **1**, we have carried out a spectroelectrochemical experiment based on

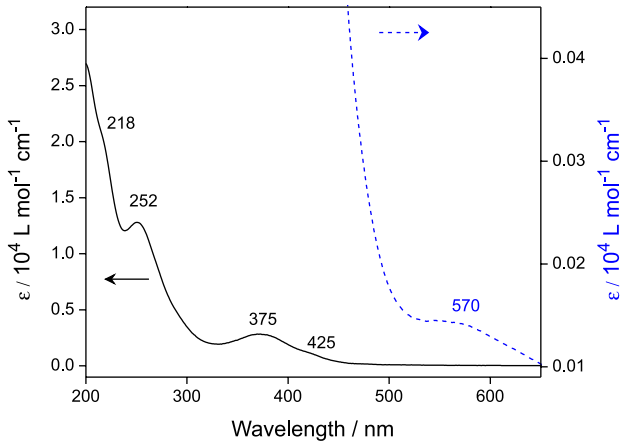

Figure 2. UV-Vis spectrum of complex **2** in acetonitrile.

EPR measurements in 0.1 mol L^{-1} $TBAPF_6$ methanolic solutions. In Figure 3a, the EPR spectra of complex **1** at 77 K showed six narrow and intense lines between 3000 and 3800 G with g = 2.0036 and isotropic hyperfine coupling constant A_o = 95.4 G typical of manganese(II) mononuclear complexes. Additionally, the spectrum of the dimeric manganese(II,II) species can be seen in the range 50-3000 G, with its clear isotropic hyperfine coupling constant signature of ca. 45 G. This can be interpreted as the sum of allowed and forbidden transitions as a result of the zero field splitting for all possible states with total spin quantum number (S_T) different from zero. According to the Clebsh-Gordan equation, S_T can assume values 5, 4, 3, 2, 1 and 0 for $S_1 = S_2 = 5/2$. Each S_T component gives rise to an EPR absorption and each absorption has an intensity given by the Boltzmann thermal factors.

Similarly to the behavior in acetonitrile, complex **1** shows a single *quasi*-reversible electrochemical process in methanol with Ep_a = 0.11 V *vs.* Ag/Ag^+. It was then electrolyzed during 30 min at 1 V under argon atmosphere and its EPR spectrum recorded at 77 K as given in Figure 3b. Under these conditions and in agreement with the similar behavior previously reported,[34] it is expected the oxidation of a single manganese center to form the mixed-valence $[Mn^{II}Mn^{III}(tidf)(OAc)(MeOH)_2]^{2+}$ complex. Coordination of methanol can strongly reduce the magnetic exchange between the Mn^{II} and Mn^{III} and, consequently, the six-line pattern seen after the oxidation can be accounted to the uncoupled Mn^{II} center of the mixed-valence compound. This is an interesting result as it relates to the magnetic behavior of the system. The EPR features also exclude the formation of Mn^{III}-Mn^{IV}, that would produce a spectrum with a spin ground S = ½ for a antiferromagnetic coupling and a very characteristic 16-line hyperfine pattern.

The other possibility is the presence of a small amount of a mononuclear Mn^{II}-tidf complex as a contaminant.

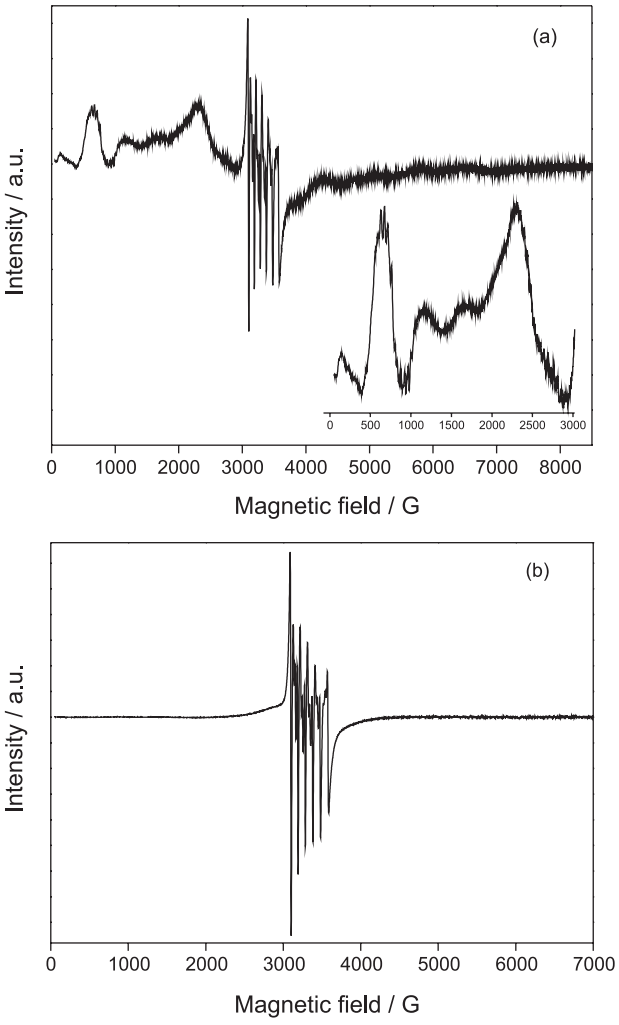

Figure 3. EPR spectra of complex **1** at 77 K in 0.10 mol L^{-1} $TBAPF_6$ in MeOH: (a) before; (b) after electrolysis in methanol at 1.0 V *vs.* Ag/Ag^+ for 30 min.

This would explain the typical six-line pattern of the EPR spectrum observed along with the broad features of the binuclear Mn(II)-Mn(II) species seen in Figure 3a. However, electrochemical oxidation at 1 V of the mononuclear Mn(II) complex would produce the mononuclear Mn^{III}-complex, that would not show any EPR signals. Romain *et al.*[35] also reported a similar behavior after the electrochemical oxidation of $[Mn^{II}(L_2)]^{2+}$ (L = 6',2''-terpyridine). In that case, an one electron oxidation in CH_3CN at 1.30 V *vs.* Ag/Ag^+ produced Mn^{III} species, but the EPR spectrum at 100 K showed a 6-line signal, which was assigned to a small amount (estimated less than 5%) of the Mn^{II} complex. However, this interpretation was discarded by the authors, since the 6-line feature could still be observed even after an exhaustive oxidation at 1.65 V.

Bearing in mind that the $tidf^{2-}$ is a diphenolate ligand, another possible sequence to account for 6-line patter of the Mn^{II} species in the EPR spectrum after oxidation,

would be the unimolecular decomposition of Mn^{III} with the concomitant formation of a phenoxyl radical: $[Mn^{III}(tidf)]^+ \rightarrow [Mn^{II}(tidf^-)]^+$. The phenoxyl radical was not detected as it possibly can react with H^+ ions from the solvent-methanol. Alternatively, the spectral pattern seen in the EPR after the electrochemical oxidation of the dimanganese(II)-complex (Figure 3b) could be due to the formation of the mixed valence trinuclear compound, $[Mn^{III}Mn^{II}Mn^{III}(tidf)_2(\mu\text{-}OAc)_2]^+$. This complex molecule was isolated and had its structure recognized by single-crystal X-ray diffraction as discussed below.

Although we cannot rule out this possibility, it seems less likely to occur because as we will present later, it has a very unusual structure and shows a high degree of tension of the coordinated macrocycle, a condition that might not exist in solution.

Magnetic properties

The variable-temperature (2-300 K) magnetic measurements were collected for powdered samples of complex **1**. The temperature dependence of molar magnetic susceptibility (χ_M) and of the $\chi_M T$ product can be seen in Figure 4. The $\chi_M T$ profile of complex **1** is typical of an antiferromagnetically coupled Mn^{II} dimer. Its 300 K value (8.57 emu K mol^{-1}) is very close to the expected one for two uncoupled high-spin Mn^{II} ions (8.75 emu K mol^{-1}), lowering to 0.69 emu K mol^{-1} at 1.8 K, suggesting the presence of an unpaired remaining Mn^{II} spin fraction. A quantitative estimation of the Mn^{II} monomeric molar fraction, as well as of the magnetic exchange constant J can be obtained through a least squares fitting procedure of the $\chi(T)$ plot. The Heisenberg-Dirac-van Vleck Hamitonian used to fit the data has been $\hat{H} = -J \cdot \hat{S}_1 \cdot \hat{S}_2$, leading to the theoretical expression for χ_M reported in the Supplementary Information.[36] The exchange interaction constant J was found to be −1.59(1) cm^{-1}, in line with literature data about structurally similar Mn^{II} dimmers.[37] Small discrepancies with experimentally determined J values for the structurally related $[Mn_2(tidf)(OAc)](ClO_4)$ complex may indicate a different mode of coordination of acetate and perchlorate ligands. Unfortunately, without the single-crystal structure for both compounds, a definite conclusion could not be unequivocally established.

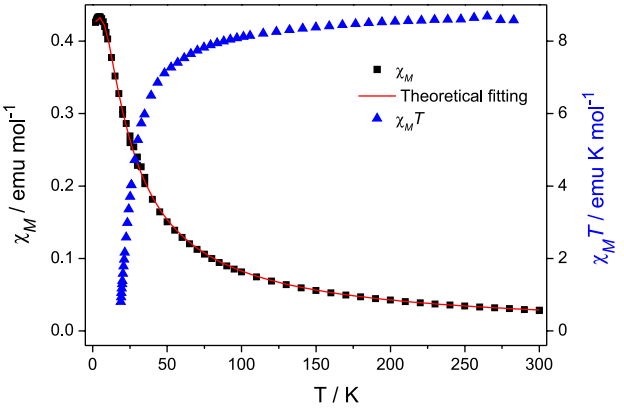

Figure 4. Magnetic susceptibility data as a function of the temperature for complex **1**. The red solid line is the best fit according to the theoretical expression discussed in the text, $R^2 = 0.999$.

Structural description of the trimanganese mixed-valence complex $[Mn_3(tidf)_2(\mu\text{-}OAc)_2](ClO_4)_2$

Figure 5 shows the representation of the molecular structure of the cation complex $[Mn_3(tidf)_2(\mu\text{-}OAc)_2]^{2+}$ that crystallized in the presence of perchlorate anions in an overall composition $C_{52}H_{58}Cl_2Mn_3N_8O_{16}$ and with molecular mass of 1287 g mol^{-1}. Many unsuccessful attempts were made to obtain single-crystals suitable for structure determination of complexes **1** and **2**. As a result of the slow diffusion of toluene into a dichloromethane solution of **1**, we were able to isolate a single batch of yellow crystals proper for diffraction. Unfortunately, the crystals were geminated and exhibited a high degree of disorder resulting in high values of R = 0.0977 and $R_w = 0.273$. Despite our efforts, we were unable to reproduce the crystallization of similar batches of the compound. Considering the unusual mode of coordination of the macrocycle ligand and, most importantly, its elevated distortion round the metal ion, apparently this is not a stable molecule and we found no experimental evidence that the complex could maintain that structure in solution.

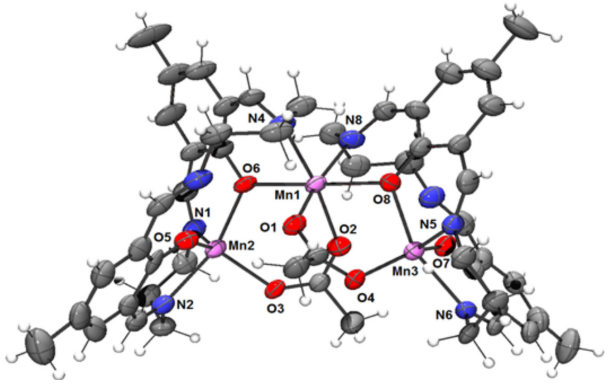

Figure 5. View of the molecular structure of $[Mn_3(tidf)_2(\mu\text{-}OAc)_2](ClO_4)_2$ with the atom-labeling scheme. Displacement ellipsoids are drawn at the 50% probability level. Perchlorate anion was omitted for clarity.

Table 2 contains main bond lengths and angles. The complex crystallizes in the triclinic space group. It is formed by two pentacoordinated units of $[Mn^{III}(tidf)]^+$ and one hexacoordinated manganese (II) core connected to each

Table 2. Selected bond lengths (Å) and angles (°) for $[Mn_3(tidf)_2(\mu\text{-}OAc)_2](ClO_4)_2$

Bond length / Å		Angle / degree			
Mn(1)-O(2)	2.158(5)	O(2)-Mn(1)-O(3)	86.1(2)	O(5)-Mn(2)-N(1)	135.1(2)
Mn(1)-O(1)	2.162(5)	O(2)-Mn(1)-O(6)	94.9(2)	O(5)-Mn(2)-N(2)	84.7(2)
Mn(1)-O(6)	2.152(4)	O(2)-Mn(1)-O(8)	84.2(2)	O(6)-Mn(2)-N(1)	83.8(2)
Mn(1)-O(8)	2.127(5)	O(2)-Mn(1)-N(4)	171.4(2)	O(6)-Mn(2)-N(2)	162.1(2)
Mn(1)-N(4)	2.231(5)	O(2)-Mn(1)-N(8)	96.9(2)	N(1)-Mn(2)-N(2)	88.0(2)
Mn(1)-N(8)	2.264(7)	O(1)-Mn(1)-O(6)	96.8(2)	O(2)-Mn(3)-O(4)	78.8(2)
Mn(2)-O(3)	2.050(3)	O(1)-Mn(1)-O(8)	87.8(2)	O(2)-Mn(3)-O(7)	73.7(2)
Mn(2)-O(5)	2.064(4)	O(1)-Mn(1)-N(4)	86.7(2)	O(2)-Mn(3)-O(8)	72.6(2)
Mn(2)-O(6)	2.108(5)	O(1)-Mn(1)-N(8)	167.0(2)	O(2)-Mn(3)-N(5)	149.2(2)
Mn(2)-N(1)	2.176(5)	O(6)-Mn(1)-O(8)	175.2(2)	O(2)-Mn(3)-N(6)	124.9(2)
Mn(2)-N(2)	2.220(7)	O(6)-Mn(1)-N(4)	81.4(2)	O(4)-Mn(3)-O(7)	145.7(2)
Mn(3)-O(4)	2.087(5)	O(6)-Mn(1)-N(8)	95.6(2)	O(4)-Mn(3)-O(8)	99.9(2)
Mn(3)-O(7)	2.087(5)	O(8)-Mn(1)-N(4)	100.2(2)	O(4)-Mn(3)-N(5)	90.2(2)
Mn(3)-O(8)	2.101(5)	O(8)-Mn(1)-N(8)	79.9(2)	O(4)-Mn(3)-N(6)	95.7(2)
Mn(3)-N(5)	2.240(5)	N(4)-Mn(1)-N(8)	91.2(2)	O(7)-Mn(3)-O(8)	91.2(2)
Mn(3)-N(6)	2.206(5)	O(3)-Mn(2)-O(5)	118.1(2)	O(7)-Mn(3)-N(6)	83.8(2)
		O(3)-Mn(2)-O(6)	104.5(2)	O(8)-Mn(3)-N(5)	81.2(2)
		O(3)-Mn(2)-N(1)	106.5(2)	O(8)-Mn(3)-N(6)	158.9(2)
		O(3)-Mn(2)-N(2)	93.1(2)	N(5)-Mn(3)-N(6)	84.5(2)
		O(5)-Mn(2)-O(6)	89.9(2)		

other through one μ-phenolate and one μ-acetate bridge. The macrocycle ligand is exceptionally distorted from its usual planar conformation. In $[Mn_3(tidf)_2(\mu\text{-}OAc)_2]^{2+}$, manganese (III) ion is five coordinated to three oxygen atoms (two from phenolates in a *cis* configuration, and one from acetate) and two iminic nitrogens. The bond distances between $Mn^{III}2$ and the oxygen atoms O3, O5, O6 (2.050(3), 2.064(5), 2.108(5) Å, respectively) are shorter than those to N1 (2.176(5) Å) and N2 (2.220(7) Å). Manganese (II) is six bonded to *trans*-phenolate O6 at 2.152(4) Å and O8 at 2.127(5) Å occupying the apical positions, while O1, O2 (acetate) and N4 and N8 (imine) are in the equatorial plane, with distances of 2.162(5), 2.158(5), 2.231(5) and 2.264(7), in that order. Angles confirm the distorted pentacoordination around the trivalent manganese ions (see for instance, O3-Mn2-05, O3-Mn2-O6, O3-Mn2-N1 and O3-Mn2-N2 at 118.1(2), 104.5(2), 106.5(2) and 93.1(2)°, in that order) and the somewhat octahedral divalent manganese (II) as given by 06-Mn1-O8, O6-Mn1-O1, O6-Mn1-N4 at 175.2(2), 96.8(2) and 81.4(2)°. This is very unique structure, because it contains two units of the macrocycle ligand tidf simultaneously bound to the hexacoordinated Mn(II) ion. As far as we know, there is no other published example of this mode of coordination using this tetraiminodiphenolate ligand.

Conclusions

The binuclear complex $[Mn^{II}_2(tidf)(OAc)(ClO_4)(MeOH)]$ (**1**) was successfully prepared by template synthesis and its spectroscopic, electrochemical and magnetic properties investigated. From the magnetic point of view, **1** showed a weak antiferromagnetic behavior ($J = -1.59(1)$ cm^{-1}) and a remaining uncoupled mononuclear Mn^{II} fraction of 3.5%. EPR signals from frozen methanolic solutions at 77 K are consistent with these findings, showing binuclear Mn^{II}-Mn^{II} to be the major compound, along with a small amount of a mononuclear Mn^{II} species. UV-Vis and EPR spectroelectrochmical responses after oxidation of complex **1** at 1 V *vs.* Ag/Ag^+ reveal oxidation and stabilization of a probable valence-trapped mixed-valence complex Mn^{II}-Mn^{III} with close resemble of spectral features of complex **2**. Crystallization of **1** produced a new and unexpected compound $[Mn_3(tidf)_2(\mu\text{-}OAc)_2](ClO_4)_2$ (**3**) containing a trinuclear and complex $Mn^{III}Mn^{II}Mn^{III}$ structure. The complex can be seen as two pentacoordinated $[Mn^{III}(tidf)]^+$ motifs connected to a central hexacoordinated Mn^{II} ion through phenolate and acetate bridges. The severe distortion and uncommon mode of coordination of the macrocyclic ligand indicates an unstable compound, only detected in the solid state as a result of the self-assembly of its components.

Acknowledgements

CNPq (process number 472996/2013-4) supported this work. F. S. N. and J. C. R. thank CNPq and CAPES for research fellowships. G.P. gratefully acknowledges the financial support from EC through the ERC Advanced Grant "MolNanoMAS". We also thank Roberta Sessoli (University of Florence) and Jaisa Fernandes Soares (UFPR) for the access to the magnetic characterization equipment.

Supplementary Information

CCDC 966873 contains the supplementary crystallographic data for this paper. These data can be obtained free of charge at www.ccdc.cam.ac.uk/conts/retrieving.html [or from the Cambridge Crystallographic Data Centre (CCDC), 12 Union Road, Cambridge CB2 1EZ, UK; fax: +44(0)1223-336033; email: deposit@ccdc.cam.ac.uk].

References

1. Robson, R.; Pilkington, N. H.; *Aust. J. Chem*. **1970**, *23*, 2225.
2. Vigato, P. A.; Tamburini, S.; *Coord. Chem. Rev*. **2004**, *248*, 1717.
3. Samulewski, R. B.; da Rocha, J. C.; Stieler, R.; Lang, E. S.; Poneti, G.; Nascimento, O. R.; Nunes, F. S.; *Polyhedron* **2011**, *30*, 1997.
4. Samulewski, R. B.; da Rocha, J. C.; Fuganti, O.; Stieler, R.; Lang, E. S.; Vaz, M. G. F.; Nunes, F. S.; *J. Mol. Struct*. **2010**, *984,* 354.
5. Raimondi, A. C.; Evans, D. J.; Nunes, F. S.; *Spectrochim. Acta, Part A* **2008**, *70*, 651.
6. Raimondi, A. C.; Evans, D. J.; Drechsel, S. M.; Hasegawa, T.; Nunes, F. S.; *Spectrochim. Acta, Part A* **2007**, *67*, 145.
7. Raimondi, A. C.; Hasegawa, T.; Evans, D. J.; *Spectrochim. Acta* **2005**, *61*, 1929.
8. Raimondi, A. C.; Hitchcock, P. B.; Leigh, G. J.; Nunes, F. S.; *J. Chem. Crystallogr*. **2004**, *34*, 83.
9. Raimondi, A. C.; Mangrich, A. S.; Franco, V. S.; Toma, H. E.; Nunes, F. S.; *Polyhedron* **2004**, *23*, 2069.
10. Raimondi, A. C.; Hitchcock, P. B.; Leigh, G. J.; Nunes, F. S.; *J. Chem. Crystallogr*. **2002**, *32*, 363.
11. Thompson, L. K.; Mandal, S. K.; Tandon, S. S.; Bridson, J. N.; Park, M. K.; *Inorg. Chem*. **1996**, *35*, 3117.
12. Gagné, R. R.; Spiro, C. L.; Smith, T. J.; Hamann, C. A.; Thies, W. R.; Shiemke, A. K.; *J. Am. Chem. Soc*. **1981**, *103*, 4073.
13. Spiro, C. L.; Lambert, L. L.; Smith, T. J.; Duesler, E. N.; Gagné, R. R.; Hendrickson, D. N.; *Inorg. Chem*. **1981**, *20*, 1229.
14. Gagné, R. R.; Henling, L. M.; Kistenmacher, T. J.; *Inorg. Chem*. **1980**, *19*, 1226.
15. Lambert, S. L.; Hendrickson, D. N.; *Inorg. Chem*. **1979**, *18*, 2683.
16. Okawa, H.; Kida, S.; *Bull. Chem. Soc. Jpn*. **1972**, *45*, 1759.
17. Coe, B. J.; Meyer, T. J.; White, P. S.; *Inorg. Chem*. **1995**, *34*, 3600.
18. Bernhardt, P. V.; Martinez, M.; *Inorg. Chem*. **1999**, *38,* 424.
19. Berhhardt, P. V.; Bozoglian, F.; Macpherson, B. P.; Martinez, M.; *Coord. Chem. Rev.* **2005**, *249*, 1902.
20. Gu, J. Z.; Kou, H. Z.; Jiang, L.; Lu, T. B.; Tan, M. Y.; *Inorg. Chim. Acta* **2006**, *359*, 2015.
21. Rodriguez-Dieguez, A.; Kivekas, R.; Sillanpaa, R.; Cano, J.; Lloret, F.; Mackee, V.; Stoeckli-Evans, H.; Colacio, E.; *Inorg. Chem*. **2006**, *45*, 10537.
22. Wen, H. R.; Wang, C.-F.; Zuo, J. L.; Song, Y.; Zeng, X. R.; You, X.-Z.; *Inorg. Chem*. **2006**, *45*, 582.
23. Wen, H.-R.; Wang, C.-F.; Song, Y.; Gao, S.; Zuo, J.-L.; You, X.-Z.; *Inorg. Chem*. **2006**, *45*, 8942.
24. Signorella, S.; Hureau, C.; *Coord. Chem. Rev*. **2012**, *256*, 1229.
25. Earnshaw, A.; *Introduction to Magnetochemistry*; Academic Press: London, 1961.
26. Bruker 2009 APEX2, SAINT and SADABS. Bruker AXS Inc., Madison, Wisconsin, USA.
27. Burla, M. C.; Caliandro, R.; Camalli, M.; Carrozzini, B.; Cascarano, G. L.; De Caro, L.; Giacovazzo, C.; Polidori, G.; Spagna, R.; *J. Appl. Crystallogr*. **2005**, *38*, 381.
28. Sheldrick, G. M.; *Acta Crystallogr., Sect. A: Found. Crystallogr.* **2008**, *64*, 112.
29. Spek, A. L.; *J. Appl. Crystallogr.* **2003**, *36*, 7.
30. Farrugia, L. J.; *J. Appl. Crystallogr*. **1997**, *30*, 565.
31. Bosnich, B.; *J. Am. Chem. Soc*. **1968**, *90*, 627.
32. Dutta, S. K.; Werner, R.; Floerke, U.; Mohanta, S.; Nanda, K. K.; Haase, W.; Nag, K.; *Inorg. Chem*. **1996**, *35*, 2292.
33. Wada, H.; Aono, T.; Motoda, K.-I.; Ohba, M.; Matsumoto, N.; Okawa, H.; *Inorg. Chim. Acta* **1996**, *246*, 13.
34. Chang, H.-R.; Larsen, S. K.; Boyd, P. D. W.; Pierpont, C. G.; Hendrickson, D. N.; *J. Am. Chem. Soc*. **1988**, *110*, 4565.
35. Romain, S.; Baffert, C.; Duboc, C.; Leprêtre, J.-C.; Deronzier, A.; Collomb, M.-N.; *Inorg. Chem*. **2009,** *48*, 3125.
36. O'Connor, C. J.; *Prog. Inorg. Chem*. **1982**, 29.
37. Luneau, D.; Savariault, J. M.; Cassoux, P.; Tuchagues, J. P.; *J. Chem. Soc., Dalton Trans.* **1988**, 1225.

Submitted on: March 15, 2014
Published online: June 10, 2014